

Quantum dynamics of the $\text{O} + \text{OH} \rightarrow \text{H} + \text{O}_2$ reaction at low temperatures

Goulven Quéméner, Naduvalath Balakrishnan

Department of Chemistry, University of Nevada Las Vegas, Las Vegas, Nevada 89154, USA

Brian K. Kendrick

Theoretical Division, Los Alamos National Laboratory, Los Alamos, New Mexico 87545, USA

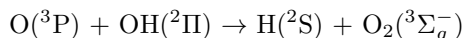
(Dated: September 14, 2021)

We report quantum dynamics calculations of the $\text{O} + \text{OH} \rightarrow \text{H} + \text{O}_2$ reaction on two different representations of the electronic ground state potential energy surface (PES) using a time-independent quantum formalism based on hyperspherical coordinates. Calculations show that several excited vibrational levels of the product O_2 molecule are populated in the reaction. Rate coefficients evaluated using both PESs were found to be very sensitive to the energy resolution of the reaction probability, especially at temperatures lower than 100 K. It is found that the rate coefficient remains largely constant in the temperature range 10 – 39 K, in agreement with the conclusions of a recent experimental study [Carty et al., *J. Phys. Chem. A* **110**, 3101 (2006)]. This is in contrast with the time-independent quantum calculations of Xu et al. [*J. Chem. Phys.* **127**, 024304 (2007)] which, using the same PES, predicted two orders of magnitude drop in the rate coefficient value from 39 K to 10 K. Implications of our findings to oxygen chemistry in the interstellar medium are discussed.

PACS numbers:

I. INTRODUCTION

The reaction



is of considerable importance in atmospheric, combustion and interstellar chemistry. In the upper stratosphere and lower mesosphere, it plays a major role in partitioning the relative abundance of OH and HO_2 molecules [1, 2, 3]. The reaction also plays a key role in the night-time air-glow emissions from the hydroxyl radical which has also been recently detected in the atmosphere of Venus [4]. It has been identified as a key reaction in interstellar oxygen chemistry [5, 6, 7] and it is considered to be the most important source of oxygen molecules in cold interstellar clouds [8, 9]. As a consequence, the HO_2 system has been the topic of numerous electronic structure calculations of its potential energy surface [10, 11, 12, 13, 14, 15] as well as dynamics calculations to evaluate its temperature dependent rate coefficients [13, 14, 16, 17, 18, 19, 20, 21, 22, 23, 24, 25, 26]. The reaction has also been the focus of a large number of experimental measurements [27, 28, 29, 30, 31, 32, 33, 34, 35, 36]. However, there still remains significant discrepancy between measured and computed values of its rate coefficients for temperatures below 200 K, which is the most important region for astrophysical and upper atmospheric applications.

Recently, Carty et al. [36] reported an experimental measurement of rate coefficients for the reaction in the temperature range 39 K to 142 K and observed no variation in the rate coefficients with temperature in this regime. Based on their findings they concluded that the rate coefficient would largely remain constant between 39 K to 10 K, temperatures typical of cold interstellar

clouds. In contrast to the experimental results of Carty et al., in a recent theoretical work using a time-independent quantum mechanical (TIQM) method and a J -shifting approximation, Xu et al. [24] reported a rate coefficient that precipitously dropped by about two orders of magnitude between 39 K and 10 K. Using a time-dependent wave packet (TDWP) method that does not employ the J -shifting approximation, Lin et al. [25] reported a rate coefficient at 10 K that is about one order of magnitude smaller than that obtained by Carty et al. at 39 K. In a subsequent study, Quan et al. [37] adopted these rate coefficients for modeling molecular oxygen chemistry in the interstellar medium.

In this paper, using an accurate TIQM method and two different representations of the electronic ground state of the HO_2 system, we show that the low temperature rate coefficient of the $\text{O} + \text{OH}$ reaction is very sensitive to the dense resonance structures in the energy dependence of its reaction probability. By using a very fine grid of collision energies in the low and ultralow regime to compute the reaction probabilities, we obtain nearly temperature independent values of the reaction rate coefficients in the range 10 – 39 K, in agreement with the conclusions of Carty et al. [36]. Our results differ from those of Xu et al. [24] which show rapid decrease below 40 K. However, our results do merge with those of Xu et al. at temperatures above 300 K where the low energy regime does not make a significant contribution. We believe that the rate coefficient reported here would provide a more accurate value for modeling oxygen chemistry in the interstellar medium.

A brief description of the computational method is provided in section II followed by results and discussion in section III. Conclusions are presented in section IV.

II. COMPUTATIONAL METHOD

The calculations have been performed using the adiabatically adjusting principal-axis hyperspherical (APH) approach of Pack and Parker [38]. In the present work, we employed two representations of the electronic ground state ($1^2A''$) of the HO_2 system. We used the XXZLG PES calculated by Xu, Xie, Zhang, Lin, and Guo [14, 15] which was also employed in the study of Xu et al. [24]. For the other surface, we used the diatomics-in-molecule (DIM) PES developed by Kendrick and Pack [12], hereafter referred to as the DIMKP PES. For each value of the total angular momentum quantum number, J , and each value of the hyperspherical radius, ρ , the wavefunction is expanded onto a basis set of adiabatic functions, which are eigenfunctions of a triatomic hyperangular Hamiltonian. The hyperangular Hamiltonian is diagonalized using an Implicitly Restarted Lanczos algorithm and a hybrid DVR/FBR primitive basis set [39]. The time-independent Schrödinger equation yields a set of differential close-coupling equations in ρ , which is solved using the log-derivative matrix propagation method of Johnson [40]. The log-derivative matrix is propagated to a matching distance where asymptotic boundary conditions are applied to evaluate the reactance matrix, K^J , and the scattering matrix, S^J . The square elements of the S^J matrix provide the state-to-state transition probabilities, P^J . The matching distance ρ_m and the number of adiabatic functions n used in the basis set are determined by optimization and extensive convergence studies. The convergence of the $J = 0$ reaction probability $P_{v=0,j=0}^{r,J=0}(E_c)$ for the $\text{O} + \text{OH}(v = 0, j = 0)$ reaction with respect to ρ_m and n is summarized in Table I for the DIMKP PES and Table II for the XXZLG PES. Based on these convergence studies, we have used $\rho_m = 26.8 a_0$ and $n = 393$ in the final production calculations.

$\rho_m (a_0)$	26.8	32.7	160.6	160.6	160.6
n	393	393	393	380	300
E_c (eV)	$P_{v=0,j=0}^{r,J=0}$				
0.001	0.7269	0.7295	0.7284	0.7284	0.7282
0.01	0.3498	0.3492	0.3490	0.3490	0.3484
0.1	0.2956	0.2956	0.2954	0.2954	0.2956
1	0.1831	0.1841	0.1825	0.1835	0.2653

TABLE I: $J = 0$ reaction probability of $\text{O} + \text{OH}(v = 0, j = 0) \rightarrow \text{H} + \text{O}_2$ for the DIMKP PES for different values of the matching distance ρ_m and the number of hyperspherical channels n at different collision energies E_c .

$\rho_m (a_0)$	26.8	32.7	160.6	160.6	160.6
n	393	393	393	380	300
E_c (eV)	$P_{v=0,j=0}^{r,J=0}$				
0.001	0.2153	0.2007	0.2081	0.2081	0.2076
0.01	0.2563	0.2570	0.2577	0.2577	0.2568
0.1	0.1816	0.1807	0.1795	0.1795	0.1792
1	0.0846	0.0846	0.0841	0.0846	0.1355

TABLE II: Same as Table I but for the XXZLG PES.

III. RESULTS AND DISCUSSION

A. Probabilities

In Fig. 1 we show the $J = 0$ reaction probabilities as a function of the collision energy computed using the DIMKP PES (upper panel) and the XXZLG PES (lower panel). The reaction probabilities calculated by Xu et al.

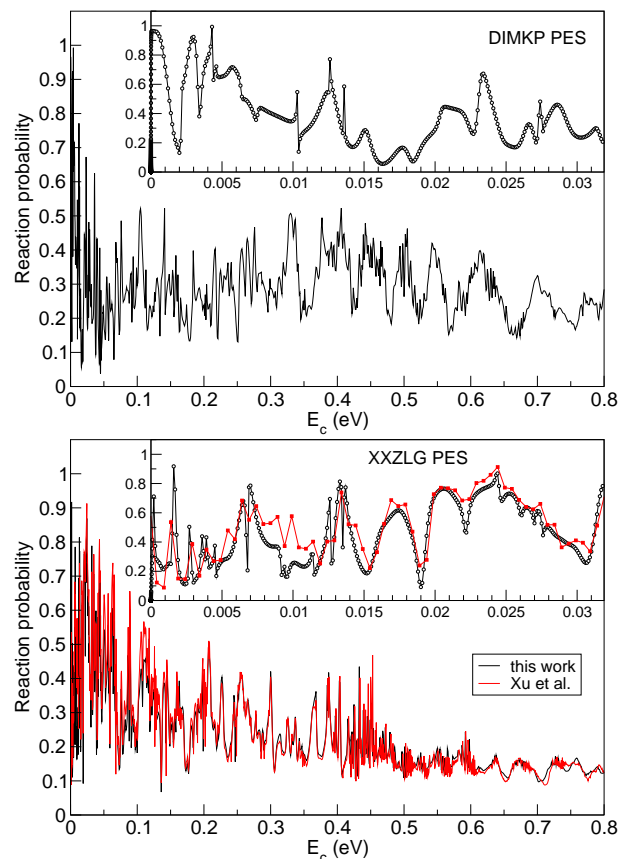


FIG. 1: (Color online) $J = 0$ reaction probabilities of $\text{O} + \text{OH}(v = 0, j = 0) \rightarrow \text{H} + \text{O}_2$ reaction on the DIMKP PES (upper panel) and the XXZLG PES (lower panel). As discussed in [41] results of Xu et al. [24] on the XXZLG PES have been shifted back by 0.00409 eV to make a one-to-one comparison with our results.

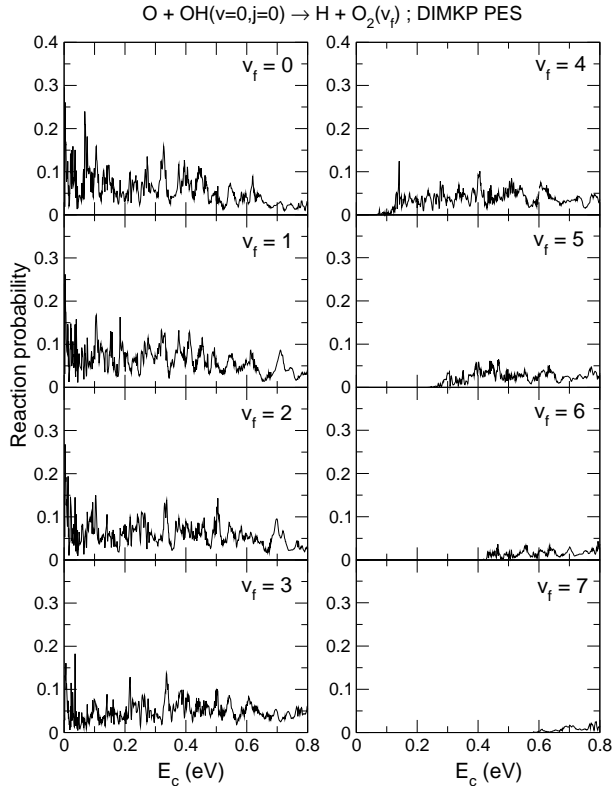


FIG. 2: Final vibrational distribution of the $J = 0$ reaction probability of $\text{O} + \text{OH}(v=0, j=0) \rightarrow \text{H} + \text{O}_2(v_f)$ for the DIMKP PES.

using the XXZLG PES and a TIQM method are also included in the lower panel. In both figures, the inset shows results for $E_c \leq 0.03$ eV to illustrate the energy resolution required for resolving the resonance features in the reaction probability. Our calculations include reaction probabilities in the energy range $E_c = [10^{-7} - 0.8]$ eV. In the energy range $E_c = [10^{-7} - 10^{-4}]$ eV where no resonance features are present we included 30 energies in a logarithmic scale. Above 0.0001 eV, we used the following energy grids: $E_c = [0.0001 - 0.0600; 0.0001]$ eV and $E_c = [0.060 - 0.800; 0.001]$ eV using linear intervals where the last number in the brackets indicates the energy spacing. The reaction probabilities obtained using the two PESs are not identical and they illustrate the sensitivity of results to details of the interaction potential. The global mean is of about 0.3 for the DIMKP PES while it is about 0.2 for the XXZLG PES. The overall trend of the reaction probabilities for the XXZLG PES is a decrease with increase in the collision energy while it oscillates around a value of about 0.3 for the DIMKP PES. The large number of resonances seen in the reaction probabilities comes from quasi-bound states of the HO_2 complex. We note that our results on the XXZLG PES are in excellent agreement with those of Xu et al. (red curves) at

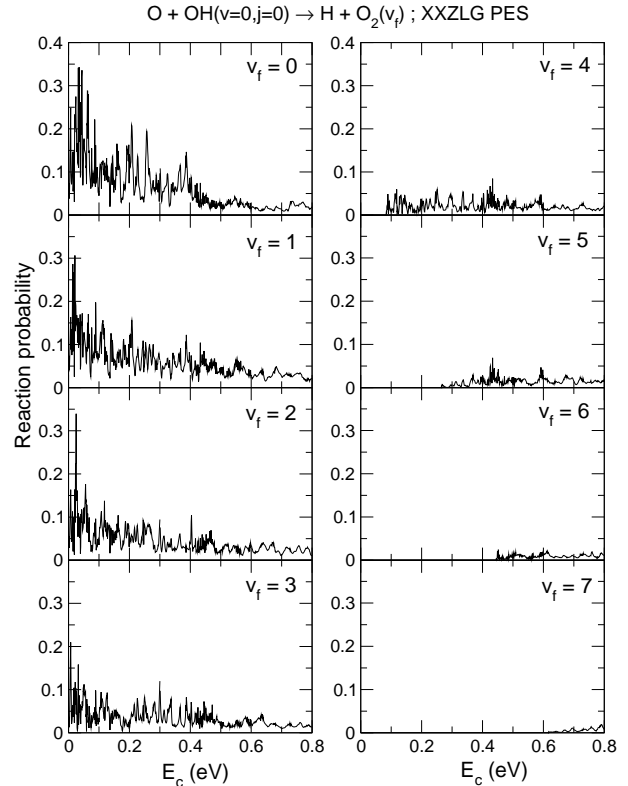


FIG. 3: Same as Fig. 2 but for the XXZLG PES.

high and intermediate collision energies. However, some discrepancies appear for low energies $E_c < 0.012$ eV as seen in the inset of the figure. As discussed in the next section, these discrepancies at the lower energies can lead to significantly different rate coefficients at low temperatures.

Since the $\text{O} + \text{OH}(v=0, j=0) \rightarrow \text{H} + \text{O}_2(v_f)$ reaction is exoergic, the reaction populates a number of excited vibrational levels of the O_2 molecule. The relative kinetic energy of the ensuing products depends on the vibrational population of the O_2 molecule. Since non-equilibrium kinetics is an important issue in upper atmospheric and astrophysical environments nascent vibrational populations of the O_2 molecules resulting from the $\text{O} + \text{OH}$ reaction will be important in modeling hydroxyl and oxygen chemistry in these environments. The computed vibrational distributions are shown in Fig. 2 for the DIMKP PES and in Fig. 3 for the XXZLG PES. The results for the DIMKP PES show that for collision energies $E_c < 0.4$ eV, O_2 molecules are formed preferentially in low-lying vibrational levels $v_f = 0 - 3$. These levels are open for the $\text{O} + \text{OH}$ reaction, even in the limit of vanishing collision energies. For collision energies $E_c > 0.4$ eV, formation of O_2 molecules in $v_f = 4, 5$ also competes with the lower vibrational levels. The re-

sults for the XXZLG PES in Fig. 3 show similar trends. Vibrational levels $v_f = 0 - 3$ are the most probable for $E_c < 0.4$ eV, while $v_f = 4, 5$ are equally probable for $E_c > 0.4$ eV. For $v_f = 0 - 3$ and $E_c < 0.4$ eV, the reaction probabilities on the XXZLG PES are larger than that of the DIMKP PES. The opposite is true for $E_c > 0.4$ eV. Overall, the reaction probabilities for a given v_f are less sensitive to the collision energy for the DIMKP PES than that of the XXZLG PES, consistent with the result for the total reaction probabilities shown in Fig. 1.

B. Rate coefficients

Accurate determination of the rate coefficients would require calculations of the reaction probabilities for all contributing values of J . Computational expense escalates quickly with J unless some angular momentum decoupling approximations are used. Like Xu et al., we use the J -shifting approximation [42] to compute the initial state-selected rate coefficients for the reaction. Within the J -shifting approximation, the rate coefficient is given by the expression:

$$k_{v,j}(T) = \frac{1}{2\pi\hbar Q_R} \times \left(\sum_J (2J+1) e^{-E_{\text{shift}}^J/(k_B T)} \right) \times \int_0^\infty P_{v,j}^{r,J=0}(E_c) e^{-E_c/(k_B T)} dE_c \quad (1)$$

where k_B is the Boltzmann constant, $P_{v,j}^{r,J=0}$ is the reaction probability and E_{shift}^J is the height of the effective barrier for a given partial wave J in the entrance channel. The barrier height is evaluated from the effective potential, V_{eff}^J , for a given partial wave:

$$V_{\text{eff}}^J = \frac{\hbar^2 J(J+1)}{2\mu(R_{\text{O-OH}})^2} + V_{\text{min}}(R_{\text{O-OH}}) \quad (2)$$

where $V_{\text{min}}(R_{\text{O-OH}})$ is the minimum energy path of the PES as a function of $R_{\text{O-OH}}$ and μ is the O–OH reduced mass. The minimum energy paths for both PESs are shown in Fig. 4. In Eq. (1), $Q_R = Q_{\text{trans}} \times Q_{\text{el}}$ is the reactant partition function. For the translational partition function we used the standard formula, $Q_{\text{trans}} = \left(\frac{\mu k_B T}{2\pi\hbar^2} \right)^{3/2}$. For the electronic partition function we used the expression given by Graff and Wagner [18]:

$$Q_{\text{el}} = \frac{(5 + 3e^{-228/T} + e^{-326/T})(2 + 2e^{-205/T})}{2}.$$

1. Sensitivity of rate coefficients to energy resolution of reaction probabilities

Calculation of rate coefficients involves integration of the Boltzmann distribution weighted by the reaction

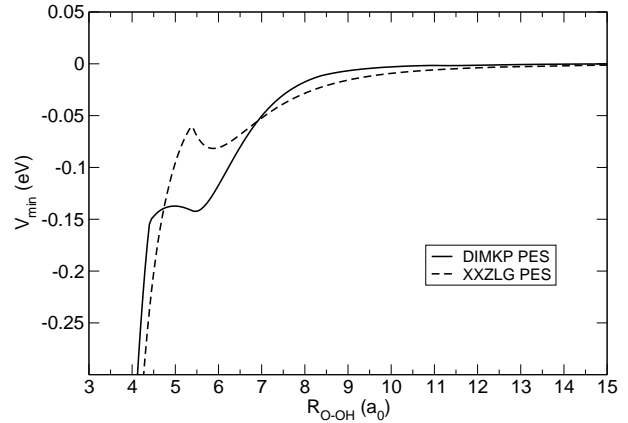


FIG. 4: Minimum energy path of the $\text{O} + \text{OH}(v=0, j=0)$ reaction as a function of $R_{\text{O-OH}}$ for the DIMKP and XXZLG PESs.

probability over the collision energy. The integration has to be performed carefully at low temperatures where the Boltzmann distribution can extend to low energies. This is especially important for capture-type reactions as the present system for which the rate coefficients are generally large at low temperatures. The typical temperature in the cold interstellar clouds is about 10 K. At this temperature, one needs to include collision energies lower than 10^{-4} eV (≈ 1 K) in accurately calculating the rate coefficients. It is known from Bethe–Wigner laws [45, 46] that rate coefficients of exothermic reactions are finite in the limit of zero temperatures [47]. The limiting value can be large for tunneling dominated reactions such as the $\text{F} + \text{H}_2$ system [47, 48] as well as barrierless reactions such as $\text{Li} + \text{Li}_2(v)$ collisions [49]. Furthermore, numerous triatomic resonances can appear in the probabilities at collision energies near the reaction threshold which can affect the value of the rate coefficient at low temperatures.

We have paid careful attention to the convergence of the reaction probabilities and rate coefficients with the resolution of collision energy grid at very low energies. Four sets of collision energies have been used to check the convergence of the rate coefficients. Fig. 5 shows the low-energy portion of the reaction probabilities employed in the four sets for the two PESs. Using the same notation as before and with the energies in eV, the first set (set 1, bold red curve) corresponds to $E_c = [0.001 - 0.800; 0.001]$. The second set (set 2, dashed green curve) includes $E_c = [0.0001 - 0.0600; 0.0005]$ and $E_c = [0.060 - 0.800; 0.001]$. The third set (set 3, thin blue curve) uses a finer energy resolution in the low energy regime: $E_c = [0.0001 - 0.0600; 0.0001]$; $E_c = [0.060 - 0.800; 0.001]$. The fourth set (set 4, dashed black curve) is composed of set 3 plus the ultralow energy regime, $E_c = [10^{-7} - 10^{-4}]$. There is no resonance fea-

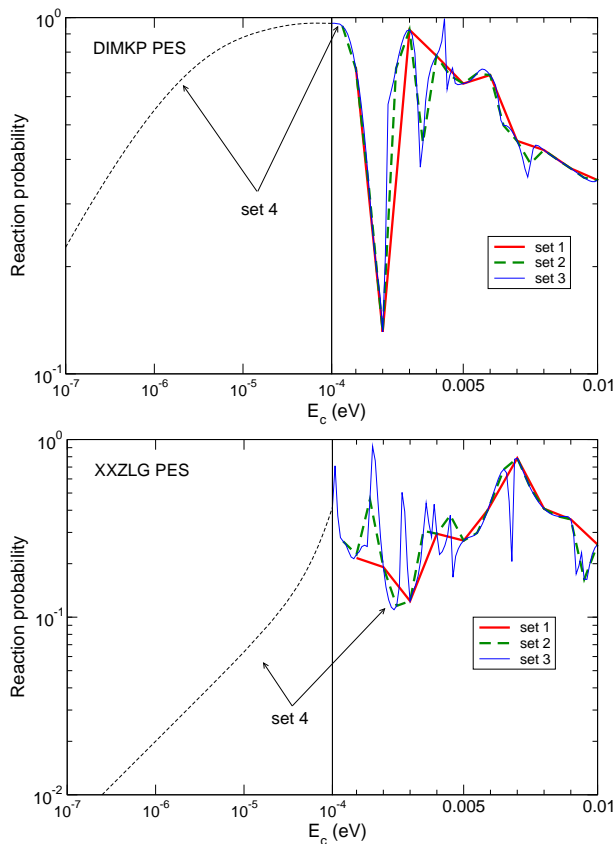


FIG. 5: (Color online) Convergence of the reaction probabilities as functions of the collision energy for the DIMKP PES (upper panel) and for the XXZLG PES (lower panel). See text for the definition of the sets employed.

tures in the ultralow energy regime where the probabilities vary as the square root of the energy, in accordance with the Bethe–Wigner laws [45, 46].

As Fig. 5 shows the ultralow regime is more prominent for the DIMKP PES due to the different description of the long-range interaction potential. It is seen that the resonances are not fully resolved in calculations with set 1 and set 2 for both PESs. This is especially the case for the XXZLG PES in the energy range 0.001 – 0.005 eV. Thus, the third multiplicative term in Eq. (1) is more accurately evaluated using set 3 and set 4.

Figure 6 shows the convergence of the rate coefficients with the energy resolution for the four collision energy sets for the DIMKP PES (upper panel) and the XXZLG PES (lower panel). The figure clearly illustrates that the rate coefficient at temperatures below 100 K are very sensitive to the resolution of the energy grid used. The convergence improves with increase in energy resolution of the reaction probabilities and also when the ultralow energy regime is included. The contribution of the ultralow energy regime is more important for the DIMKP PES as evident from the corresponding reaction probabilities shown in Fig. 5. Figure 6 shows that careful at-

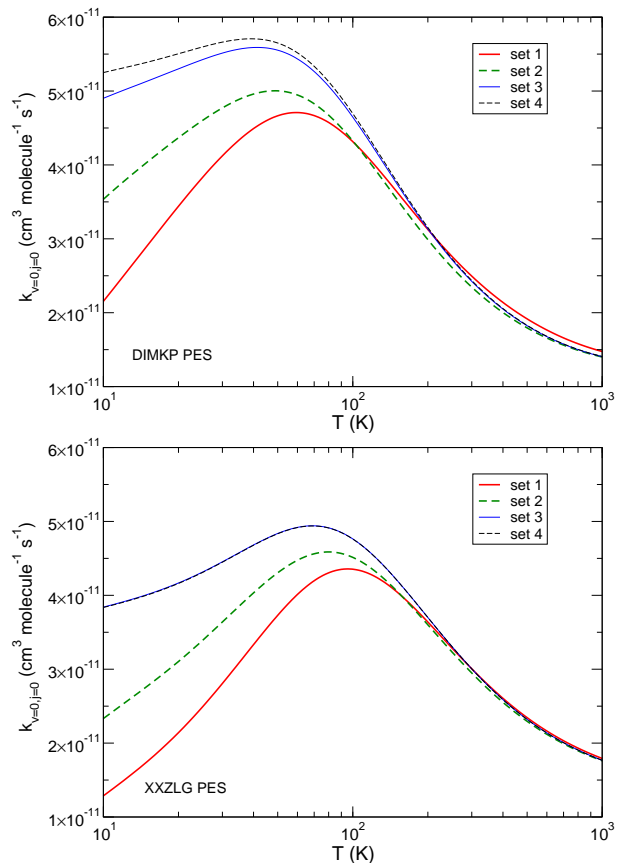


FIG. 6: (Color online) Same as Fig. 5 but for the rate coefficients as functions of the temperature.

tention must be devoted to the resolution of the energy grid and/or to the inclusion of the very low energy regime in order to accurately calculate the low temperature rate coefficients of the O + OH reaction. This applies regardless of whether or not a J -shifting approximation is used in the calculation of the rate coefficients.

2. Comparison with experiments and other theoretical results

The converged rate coefficients (results from set 4 above) for the $v = 0, j = 0$ initial state obtained from the DIMKP and the XXZLG PESs are shown in Fig. 7 as functions of the temperature along with experimental data from several groups [29, 32, 36] as well as the recommended values by NASA [43] and IUPAC [44]. The theoretical results of Xu et al. [24] obtained using the XXZLG PES and the results of Harding et al. [23] obtained using the PES of Troe and Ushakov [13] are also included for comparison. Table III lists rate coefficients at selected temperatures from different theoretical and experimental studies.

Fig. 7 shows that the XXZLG PES yields results in somewhat better agreement with the exper-

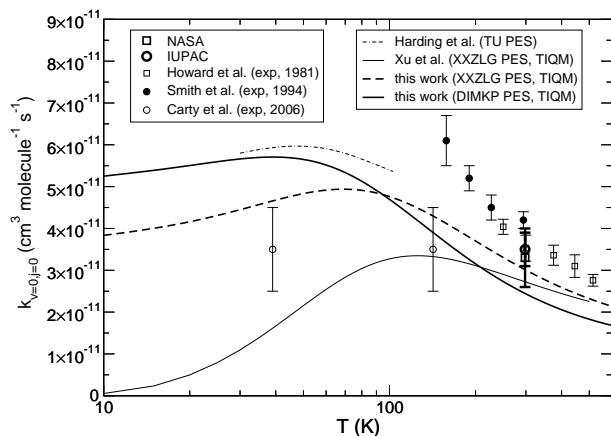


FIG. 7: Rate coefficients of $\text{O} + \text{OH}(v = 0, j = 0) \rightarrow \text{H} + \text{O}_2$ as functions of the temperature.

iments than the DIMKP PES. At $T = 298$ K, the rate coefficient calculated using the XXZLG PES is $3.01 \times 10^{-11} \text{ cm}^3 \text{ molecule}^{-1} \text{ s}^{-1}$ compared to $2.45 \times 10^{-11} \text{ cm}^3 \text{ molecule}^{-1} \text{ s}^{-1}$ obtained using the DIMKP PES. The result on the XXZLG PES is within the reported error bars of the NASA panel recommended value of $3.3 \pm 0.7 \times 10^{-11} \text{ cm}^3 \text{ molecule}^{-1} \text{ s}^{-1}$ at 298 K. The computed results on the DIMKP and XXZLG PESs lie within the quoted error bars of Carty et al. at $T = 142$ K. At $T = 39$ K, the result of the XXZLG is slightly above the experimental result, while it is higher for the DIMKP PES.

The temperature dependence of the rate coefficients predicted by the two PESs is quite similar. They predict rate coefficients within about 30% for $10 < T < 100$ K with the DIMKP PES yielding higher values. This can be explained by the energy dependence of the reaction probabilities shown in the insets of Fig. 1. The reaction probabilities are somewhat higher for the DIMKP PES than for the XXZLG PES between $0 - 0.01$ eV ($\approx 0 - 100$ K), leading to an increase in the third multiplicative term in Eq. (1). This can also be explained by the topology of the PESs. As shown in Fig. 4, the minimum energy path, $V_{\min}(R_{\text{O-OH}})$, of the DIMKP PES features a small “reef” at $R_{\text{O-OH}} = 5.0 a_0$. It is located at $R_{\text{O-OH}} = 5.4 a_0$ for the XXZLG PES. For the latter PES the reef is about 0.08 eV higher than that of the DIMKP PES. The location and height of the reef is sensitive to the electronic structure method employed. For certain values of J , it becomes an effective barrier. The smaller reef for the DIMKP PES leads to smaller effective barriers especially for higher J values. This enhances the second multiplicative term in Eq. (1) and leads to a higher rate coefficient for the DIMKP PES. For $T > 100$ K, the two PESs predict rate coefficient within 20% with the DIMKP PES yielding smaller values. This is attributed to the smaller overall reaction probabilities of the DIMKP PES compared to the XXZLG PES for $E_c > 0.01$ eV (≈ 100 K), as seen in the insets of Fig. 1.

Our computed rate coefficients do not show a significant decrease between 142 K and 39 K, consistent with the experimental results of Carty et al. [36]. Though no experimental data are available for temperatures below 39 K, our results on both PESs do not predict a dramatic decrease between 39 K and 10 K. At 10 K we obtain a rate coefficient of $3.91 \times 10^{-11} \text{ cm}^3 \text{ molecule}^{-1} \text{ s}^{-1}$ on the XXZLG PES and $5.25 \times 10^{-11} \text{ cm}^3 \text{ molecule}^{-1} \text{ s}^{-1}$ on the DIMKP PES. Our results are about a factor of 70 larger than the value of $5.41 \times 10^{-13} \text{ cm}^3 \text{ molecule}^{-1} \text{ s}^{-1}$ reported by Xu et al. [24] using the XXZLG PES and the same J -shifting approximation. The discrepancy is attributed to the sparse energy grid, small differences in the reaction probabilities for $E_c < 0.012$ eV, and the artificial energy shift in the calculations of Xu et al. [41, 50]. Among these, the energy shift is the main source of the discrepancy. Based on our results, we believe that the rate coefficients calculated by Xu et al. may not be appropriate for modeling oxygen chemistry in the interstellar medium [37]. While an accurate calculation of the rate coefficient would require the inclusion of many higher angular momentum quantum numbers and non-adiabatic couplings, the present study shows that special attention must be given to the energy grid in the calculation of low temperature rate coefficients for capture reactions.

reference	10 K	39 K	142 K	298 K
this work, DIMKP	5.25	5.71	3.90	2.45
this work, XXZLG	3.91	4.66	4.30	3.01
Xu et al. [24], XXZLG	0.0541			
Lin et al. [25], XXZLG	0.784			
Carty et al. [36]	3.5 ± 1.0		3.5 ± 1.0	
NASA [43]				3.3 ± 0.7
IUPAC [44]				3.5 ± 0.4

TABLE III: Rate coefficients of $\text{O} + \text{OH} \rightarrow \text{H} + \text{O}_2$ in units of $10^{-11} \text{ cm}^3 \text{ molecule}^{-1} \text{ s}^{-1}$ for different temperatures.

IV. CONCLUSION

In conclusion, we have performed quantum dynamics of the $\text{O} + \text{OH} \rightarrow \text{H} + \text{O}_2$ reaction over a wide range of collision energies on two recent PESs using a time-independent quantum formalism based on hyperspherical coordinates. We report total and product vibrational state-selected reaction probabilities, and initial state-selected rate coefficients for the reaction. Special attention has been devoted to the convergence of the rate coefficients with respect to the energy resolution of reaction probabilities and the inclusion of the ultralow energy regime. The computed rate coefficients are in reasonable agreement with experimental measurements and existing recommended values, despite using a J -shifting approximation for the evaluation of the rate coefficients. Our

calculations show that omission of the low energy regime or insufficient energy resolution of the reaction probabilities can lead to significant errors in the computed rate coefficients. The rate coefficient at 10 K differ by a factor of 2-3 between calculations using a finer energy grid and a sparse energy grid. Therefore, we expect that a careful choice of the energy grid will also be important for an accurate evaluation of the rate coefficients without the J -shifting approximation. Overall, results on the XX-ZLG PES are in better agreement with the experimental results of Carty et al. [36] compared to the DIMKP PES in the temperature range of 39–142 K. However, only two data points are available from measurements in this temperature range and experimental error bars are also quite large. For both PESs, the rate coefficients decrease only slightly as the temperature is decreased from 39 K to 10 K, in agreement with the conclusions of Carty et al. Based on the present results we believe that a re-evaluation of the importance of the $O + OH$ reaction on

O_2 abundance would be required for describing oxygen chemistry in the interstellar medium.

V. ACKNOWLEDGMENTS

This work was supported by NSF grants #PHY-0555565 (N.B.) and #ATM-0635715 (N.B.). B.K.K. acknowledges that part of this work was done under the auspices of the US Department of Energy at Los Alamos National Laboratory. Los Alamos National Laboratory is operated by Los Alamos National Security, LLC, for the National Nuclear Security Administration of the US Department of Energy under contract DE-AC52-06NA25396. We thank D. Xie for providing us the XX-ZLG PES, and P. Honvault for providing us the reaction probabilities and the rate coefficient obtained by Xu et al., and for helpful discussions.

-
- [1] D. C. Clary, *Mol. Phys.* **53**, 3 (1984).
- [2] M. E. Summers, R. R. Conway, D. E. Siskind, M. H. Stevens, D. Offermann, M. Riese, P. Preusse, D. F. Strobel and J. M. Russell III, *Science* **277**, 1967 (1997).
- [3] Y. P. Lee and C. J. Howard, *J. Chem. Phys.* **77**, 756 (1982).
- [4] G. Piccioni et al., *A & A* **483**, L29 (2008).
- [5] A. Dalgarno and J. H. Black, *Rep. Prog. Phys.* **39**, 573 (1976).
- [6] A. F. Wagner and M. M. Graff, *ApJ* **317**, 423 (1987).
- [7] M. M. Graff and A. Dalgarno, *ApJ* **317**, 432 (1987).
- [8] S. Viti, E. Roueff, T. W. Hartquist, G. Pineau des Forêts, and D. A. Williams, *A & A* **370**, 557 (2001).
- [9] I. W. M. Smith, *Chem. Rev.* **103**, 4549 (2003).
- [10] C. F. Melius and R. J. Blint, *J. Chem. Phys. Lett.* **64**, 183 (1979).
- [11] M. R. Pastrana, L. A. M. Quintales, J. Brandão, and A. J. C. Varandas, *J. Phys. Chem.* **94**, 8073 (1990).
- [12] B. Kendrick and R. T Pack, *J. Chem. Phys.* **102**, 1994 (1995).
- [13] J. Troe and V. G. Ushakov, *J. Chem. Phys.* **115**, 3621 (2001).
- [14] C. Xu, D. Xie, D. H. Zhang, S. Y. Lin, and H. Guo, *J. Chem. Phys.* **122**, 244305 (2005).
- [15] D. Xie, C. Xu, T.-S. Ho, H. Rabitz, G. Lendway, S. Y. Lin, and H. Guo, *J. Chem. Phys.* **126**, 074315 (2007).
- [16] J. A. Miller, *J. Chem. Phys.* **84**, 6170 (1986).
- [17] J. Davidsson and G. Nyman, *Chem. Phys.* **125**, 171 (1988).
- [18] M. M. Graff and A. F. Wagner, *J. Chem. Phys.* **92**, 2423 (1990).
- [19] A. J. C. Varandas, J. Brandão, and M. R. Pastrana, *J. Chem. Phys.* **96**, 5137 (1992).
- [20] T. C. Germann and W. H. Miller, *J. Phys. Chem. A* **101**, 6358 (1997).
- [21] D. E. Skinner, T. C. Germann, and W. H. Miller, *J. Phys. Chem. A* **102**, 3828 (1998).
- [22] A. Viel, C. Leforestier, and W. H. Miller, *J. Chem. Phys.* **108**, 3489 (1998).
- [23] L. B. Harding, A. I. Mergoiz, J. Troe, and V. G. Ushakov, *J. Chem. Phys.* **113**, 11019 (2000).
- [24] C. Xu, D. Xie, P. Honvault, S. Y. Lin, and H. Guo, *J. Chem. Phys.* **127**, 024304 (2007).
- [25] S. Y. Lin, H. Guo, P. Honvault, C. Xu, and D. Xie, *J. Chem. Phys.* **128**, 014303 (2008).
- [26] M. Jorfi, P. Honvault, P. Halvick, S. Y. Lin, and H. Guo, *Chem. Phys. Lett.* **462**, 53 (2008).
- [27] R. S. Lewis and R. T. Watson, *J. Phys. Chem.* **84**, 3495 (1980).
- [28] M. J. Howard and I. W. M. Smith, *Chem. Phys. Lett.* **69**, 40 (1980).
- [29] M. J. Howard and I. W. M. Smith, *J. Chem. Soc., Faraday Trans.* **277**, 997 (1981).
- [30] N. Cohen and K. R. Westberg, *J. Phys. Chem. Ref. Data* **12**, 531 (1983).
- [31] K. S. Shin and J. V. Michael, *J. Chem. Phys.* **95**, 262 (1991).
- [32] I. W. M. Smith and D. W. A. Stewart, *J. Chem. Soc., Faraday Trans.* **90**, 3221 (1994).
- [33] D. L. Baulch, et al., *J. Phys. Chem. Ref. Data* **23**, 847 (1994).
- [34] R. Robertson and G. P. Smith, *Chem. Phys. Lett.* **358**, 157 (2002).
- [35] R. Robertson and G. P. Smith, *J. Phys. Chem. A* **110**, 6673 (2006).
- [36] D. Carty, A. Goddard, S. P. K. Kohler, I. R. Sims, and I. W. M. Smith, *J. Phys. Chem. A* **110**, 3101 (2006).
- [37] D. Quan, E. Herbst, T. J. Millar, George E. Hassel, S. Y. Lin, H. Guo, P. Honvault, and D. Xie, *ApJ* **681**, 1318 (2008).
- [38] R. T Pack and G. A. Parker, *J. Chem. Phys.* **87**, 3888 (1987).
- [39] B. K. Kendrick, R. T Pack, R. B. Walker, and E. F. Hayes, *J. Chem. Phys.* **110**, 6673 (1999).
- [40] B. R. Johnson, *J. Comp. Phys.* **13**, 445 (1973).
- [41] The reaction probabilities reported by Xu et al. [24] were artificially shifted by 0.00409 eV (P. Honvault, private communication).

- [42] J. M. Bowman, *J. Phys. Chem.* **95**, 4960 (1991).
- [43] S. P. Sander, A. R. Ravishankara, D. M. Golden, C. E. Kolb, M. J. Kurylo, R. E. Huie, V. L. Orkin, M. J. Molina, G. K. Moortgat, and B. J. Finlayson-Pitts, Chemical kinetics and photochemical data for use in atmospheric studies. Evaluation no. 14, Jet Propulsion Laboratory, Pasadena, CA, 2003. Available from: <http://jpldataeval.jpl.nasa.gov>.
- [44] R. Atkinson, D. L. Baulch, R. A. Cox, J. N. Crowley, R. F. Hampson, R. G. Hynes, M. E. Jenkins, M. J. Rossi and J. Troe, *Atmos. Chem. Phys.* **4**, 1461 (2004). Available from: <http://www.iupac-kinetic.ch.cam.ac.uk>.
- [45] H. A. Bethe, *Phys. Rev.* **47**, 747 (1935).
- [46] E. P. Wigner, *Phys. Rev.* **73**, 1002 (1948).
- [47] P. F. Weck and N. Balakrishnan, *Int. Rev. Phys. Chem.* **25**, 283 (2006).
- [48] N. Balakrishnan and A. Dalgarno, *Chem. Phys. Lett.* **341**, 652 (2001).
- [49] G. Quémener, J.-M. Launay, and P. Honvault, *Phys. Rev. A* **75**, 050701(R) (2007), and references therein.
- [50] The rate coefficients reported in the work of Xu et al. [24] do not take into account the correction pointed out in [41]. This affects the values of the rate coefficients for $T < 50$ K and is partly responsible for the discrepancy with our results.